Superdiffusion in two-dimensional Yukawa liquids

Bin Liu and J. Goree
Department of Physics and Astronomy, The University of Iowa, Iowa City, Iowa 52242, USA
(Received 31 May 2006; published 18 January 2007)

Superdiffusion of two-dimensional (2D) liquids was studied using an equilibrium molecular dynamics simulation. At intermediate temperatures, the mean-squared displacement, probability distribution function (PDF), and velocity autocorrelation function (VACF) all indicate superdiffusion; the VACF has a long-time tail; and the PDF indicates no Lévy flights. These effects are predicted to occur in 2D dusty plasmas and other 2D liquids that can be modeled with a long-range repulsive potential.

DOI: 10.1103/PhysRevE.75.016405 PACS number(s): 52.27.Gr, 66.10.Cb, 52.27.Lw, 82.70.Dd

I. INTRODUCTION

There are many two-dimensional (2D) physical systems, some of them at a macroscopic scale, that can be in an ordered (solid) or disordered state (liquid). These include a Wigner lattice of electrons on the surface of liquid helium [1], an array of vortices in the mixed state of type-II superconductors [2,3], colloidal suspensions [4], ions confined magnetically in a Penning trap [5], and dusty plasmas levitated in a monolayer [6]. There are also physical systems with a monolayer of particles or clusters that interact not only amongst themselves, but also with an underlying substrate, such as an atomically flat surface [7]. Brown's original observation of Brownian motion was for a 2D system of small particles on a water surface [8].

Here we investigate random motion in 2D equilibrium liquids. We are motivated by a long-standing controversy over diffusion in 2D liquids, with conflicting theoretical and simulation results. In general, motion has been predicted theoretically to be nondiffusive in 2D liquids, regardless of the pair potential [9,10]; and early molecular dynamics (MD) simulations [11] with hard-disks came to a similar prediction. However, normal diffusion was detected in more recent simulations with softer potentials [12–15].

We are also motivated by recent experimental results for diffusion in 2D dusty plasma. One experimental group [16] using a quasi-2D dusty plasma claimed to observe superdiffusion, as did a second group [17] using a monolayer dusty plasma cluster in a partly ordered state that allows hydrodynamical vortical flows. However, a third group [6] with a 2D monolayer dusty plasma claimed to observe no superdiffusive motion. Superdiffusion is random motion much like normal diffusion, but it differs from normal diffusion by having larger displacements as well as distinctive signatures in correlation functions and probability distribution functions, as explained later. The two experiments with a monolayer [6,17] have a pair potential that is Yukawa [18].

Here we report results from an equilibrium MD simulation for particles interacting with a Yukawa potential and constrained to moving on a plane. We characterize the nondiffusive motion, and we find that it is superdiffusion that does not arise from Lévy flights; instead, it seems to arise from hydrodynamic modes, as indicated by a long-time tail in the velocity autocorrelation function (VACF). We note that the Yukawa system in 3D, unlike in 2D, has only been reported to exhibit diffusive motion [19]. Our results will be helpful in understanding recent experiments with 2D dusty plasmas [6,17]. They will be helpful also for gaining an understanding of other experimental systems with long-range repulsive potentials, including pure-ion plasmas, electrons on the surface of liquid helium, and microspheres in a colloidal suspension.

II. SIMULATIONS

We performed equilibrium MD simulations. We used the Yukawa pair potential, $\phi(r)=Q^2\exp(-r/\lambda_D)/4\pi\epsilon_0 r$, where Q is particle charge and λ_D is screening length. Equilibrium Yukawa systems can be classified completely by the values of Γ and κ [19,20]. Here, $\Gamma=Q^2/4\pi\epsilon_0 a k_B T$ and $\kappa\equiv a/\lambda_D$, where T is particle kinetic temperature, $a\equiv(n\pi)^{-1}$ is the Wigner-Seitz radius [21], and n is the areal number density. Time scales of interest are characterized by $\omega_{pd}^{-1}=(Q^2/2\pi\epsilon_0 m a^3)^{-1/2}$, where m is particle mass. Another parameter of interest is T/T_m, where the melting temperature T_m depends on κ and has a value of $T_m\approx 145$ for $\kappa=0.56$ [22]. In this paper, we investigate the intermediate-temperature regime $5<\Gamma<88$, identified in [23] as having nondiffusive motion. We assume $\kappa=0.56$, comparable to the value in 2D dusty plasma experiments [6].

Our simulation is similar to the monolayer dusty plasma experiments [6,17] in the use of a 2D monolayer with a Yukawa potential and similar values of parameters Γ and κ, but it differs from these experiments in three ways. It describes a frictionless atomic system, it uses periodic boundary conditions to model an infinite system, and it models an equilibrium situation without instabilities driven by ion flow.

In our simulation, we integrate the equation of motion of N particles. We used $N=1024$, and we verified that our results are independent of N over a range from 1024 to 16 384. We repeated our simulations for six different initial configurations of the particle positions, averaging these results to improve the statistics. A Nosé-Hoover thermostat is applied to control the temperature. Further details of the simulation method, along with further tests of its validity, were reported in [23,24]. Among other considerations, a simulation must use a sufficiently short time step to conserve energy and an adequately large box size to allow computing meaningful quantity at long times. The required box size is generally the desired maximum time multiplied by the sound speed for ordered liquids or ballistic particle speed for gases.

III. SELF-DIFFUSION

We use three diagnostics to characterize particle motion. We found they are consistent with one another when classifying the motion as diffusive or superdiffusive. However, investigators may differ in their classification, depending on their system size, which is related to the time range where data can be evaluated, and qualitative judgments of the appearance of a curve.

The first diagnostic, mean-squared displacement (MSD), $\langle|\mathbf{r}_i(t)-\mathbf{r}_i(0)|^2\rangle$, is the most common. Here, $r_i(0)$ is the initial position of particle i. Normal diffusion, i.e., Fickian diffusion, can be identified when the MSD scales linearly with time t, while for superdiffusion MSD increases more rapidly. When graphed as a function of time in a log-log plot, if the curve fits a straight line with a slope α, then the MSD obeys a power low $\propto t^{\alpha}$. Normal diffusion is characterized by $\alpha=1$, while superdiffusion and subdiffusion have larger and smaller slopes, respectively. Most authors mention $\alpha=1$ as a criterion for classifying motion as diffusive, but in practice this is not useful because actual empirical data will never yield exactly a slope of unity. While most investigators do not apply a numerical criterion, we follow the prescription of Feder *et al.* [25]: a range of $0.9<\alpha<1.1$ is classified as diffusive motion.

Here, we also make a stricter test of the MSD curve using the prediction of the Stokes-Einstein relation. We combine three relations: the Stokes-Einstein relation $D=k_BT/1.69\pi\eta$ [23], which relates the shear viscosity coefficient η and diffusion constant D; the Einstein relation $\lim_{t\to\infty}\langle|\mathbf{r}(t)-\mathbf{r}(0)|^2\rangle=4Dt$; and the Green-Kubo relation for computing η from simulation data. This method assumes a valid viscosity coefficient exists, which has been verified in [24,26]. Thus, the value of D predicted in this way can be used to compute predicted MSD data, which can be compared to the simulation MSD data to determine whether the value of D is valid and therefore determine whether the motion is actually diffusive. This test is stricter than relying solely on the slope α because it makes use of both the slope and the intercept.

The second diagnostic, PDF, is the probability distribution function, which is a histogram of the squared displacement $(\Delta r)^2$ made by particles as compared to their initial positions. Diffusive motion is characterized by a PDF that is Gaussian; in contrast, motion that obeys Lévy statistics is characterized by a PDF that has an inverse power law [27]. The PDF is therefore useful for identifying whether superdiffusion is due to Lévy statistics, as was claimed for the experiment of [17].

The third diagnostic, VACF, is the ensemble average of the product of particle velocities at time t and an earlier time 0. The VACF is computed as $\langle\mathbf{v}_i(t)\cdot\mathbf{v}_i(0)\rangle/2$. If the motion is normal diffusion, the VACF will decay much faster than $1/t$, and a valid diffusion coefficient can be computed as the integral, i.e., the area under the VACF, using the Green-Kubo relation [28]. On the other hand, if motion is superdiffusive, the VACF will decay much more slowly, typically as $1/t$, and the integral diverges due to this long-time tail. If the VACF oscillates and has an integral that tends to zero, the motion is identified as subdiffusive. The VACF is most useful at higher temperatures, well above melting, whereas at lower temperatures it has oscillations that hinder identifying the scaling of a long-time tail. For this reason, at low temperatures the MSD or PDF can be more useful than the VACF.

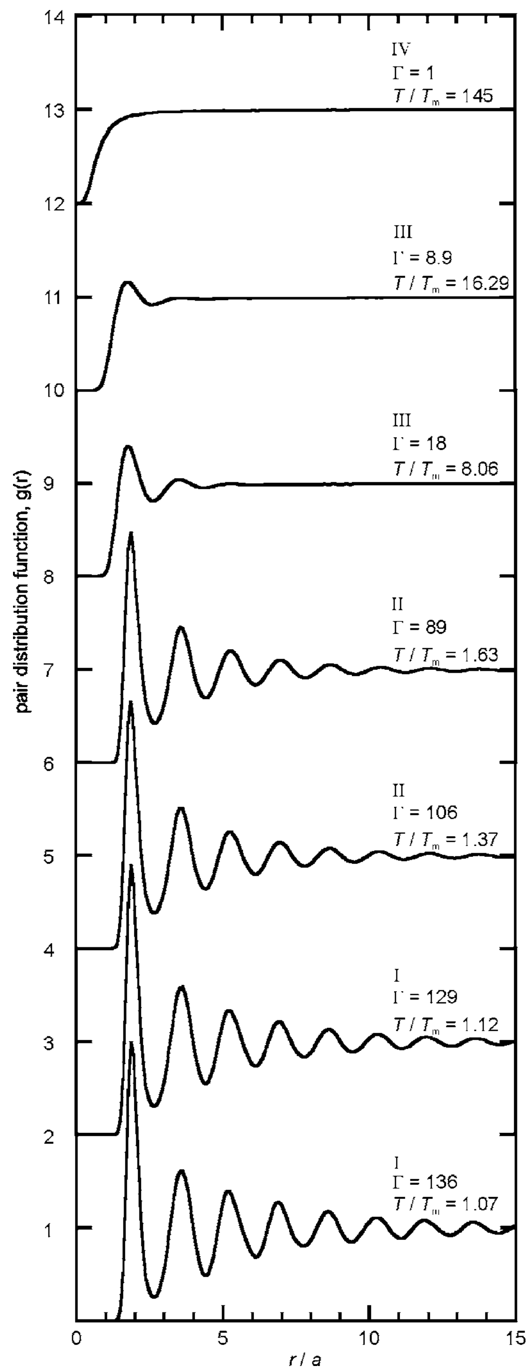

FIG. 1. Pair correlation function $g(r)$ from our MD simulation, for some of the values of Γ reported in this paper. The states varied from a nonideal gas at $\Gamma=1$ to a strongly coupled liquid at $\Gamma=136$. Temperatures here are normalized by T_m as reported by Hartmann *et al.* [22].

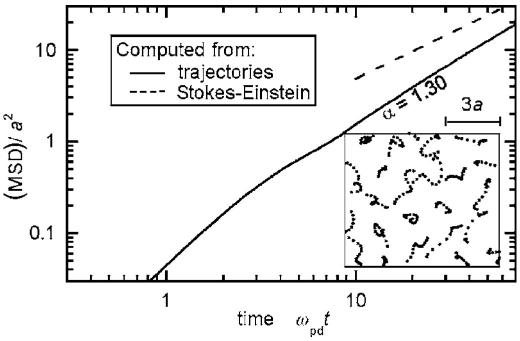

FIG. 2. Mean-squared displacement MSD. Simulation results are shown as a solid line. Superdiffusion is indicated by a slope $\alpha > 1$, and by an MSD below the dashed line except at very long time. The dashed line is a prediction based on a combination of the Stokes-Einstein relation, the Einstein relation, and the viscosity computed in [24] from the Green-Kubo relation. Note that the system shown here at $\Gamma=18$ and $\kappa=0.56$ is a disordered liquid, as shown by particle trajectories in the inset for a period of $0 < \omega_{pd}t < 10$. Distance is normalized by the Wigner-Seitz radius a.

IV. RESULTS

This simulation studies disordered Yukawa liquids, covering from nonideal gases to near disordering transition strongly coupled liquid. As a measurement of the order or disorder of the liquid, we present the pair correlation function, $g(r)$, in Fig. 1. This is useful to allow the reader to compare our results, for a given value of Γ and κ, to other authors' results for different values of these parameters (or even a different potential) provided that $g(r)$ appears similar.

A. Superdiffusive case, $\Gamma=18$

Results for the MSD, in Fig. 2, show that the motion is superdiffusive, for $\Gamma=18$. Here we are interested in motion for $\omega_{pd}t \gg 1$. (At shorter times the motion is ballistic, as a particle moves inside the cage formed by neighboring particles.) We find that the MSD grows faster than linearly, as compared to the MSD calculated by using the Stokes-Einstein relation. First, in the most common test of superdiffusion, here we find that the slope α is greater than unity. Calculating the exponent,

$$\alpha = \frac{d[\log\langle|\mathbf{r}_i(t) - \mathbf{r}_i(0)|^2\rangle]}{d[\log t]} \tag{1}$$

and averaging this value in the range $30 < \omega_{pd}t < 70$, we find $\alpha=1.30$ for $\Gamma=18$. Moreover, comparing the simulation results to the dashed line in Fig. 2 predicted by using Stokes-Einstein relation, we find a noticeable deviation. Both of these findings, $\alpha > 1$ and an MSD curve that deviates from the prediction of the Stokes-Einstein relation, indicate that the motion is superdiffusion.

Results for the PDF, Fig. 3, indicate that the motion is superdiffusive. Instead of plotting the PDF vs $(\Delta r)^2$, here we plot it vs $(\Delta r)^2/t$. If motion were diffusive, the data would fall on a universal curve. For the intermediate-temperature regime studied here, we found that the data never fall on a universal curve, so that we identify the motion as nondiffusive. In particular, the data fall on a line with a slope that becomes less steep with time, as in Fig. 3(a) for $\Gamma=18$, and this is an indication of superdiffusion. For comparison, we also show in Fig. 3(b) the PDF for the different regime of a cold liquid, $\Gamma=106$, where the data fall on a universal curve for $\omega_{pd}t > 10$.

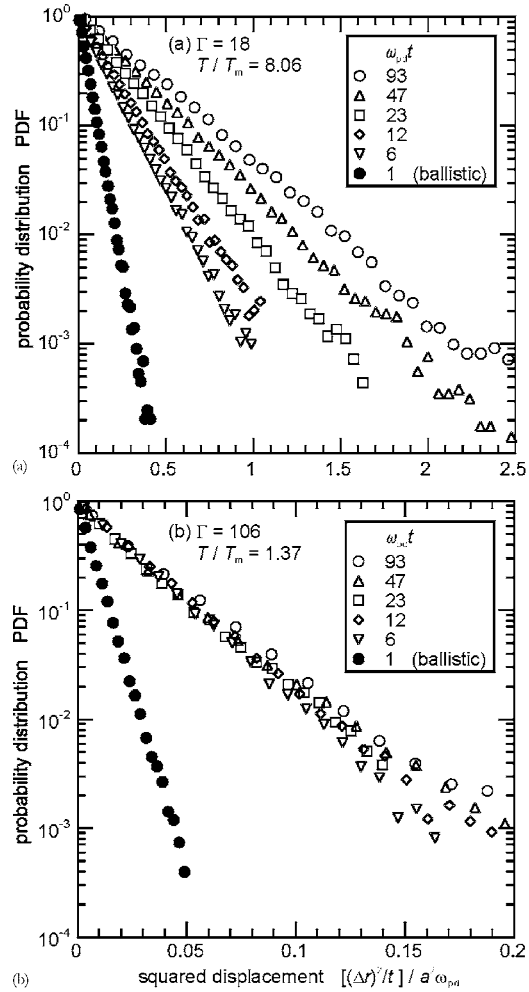

FIG. 3. Probability distribution function, PDF. This is a histogram of the squared displacement $(\Delta r)^2$ made by a particle during a measurement interval t. A straight line in this semilogarithmic graph indicates a Gaussian PDF, which rules out Lévy statistics. (a) In the intermediate-temperature regime, the width of the Gaussian increases faster than t, indicating superdiffusion. (b) In a cold liquid, data for $\omega_{pd}t > 10$ fall on a universal curve, indicating diffusive motion or much less extreme superdiffusion. Motion for $\omega_{pd}t < 10$ corresponds to ballistic motion, which is not of interest when classifying random motion as diffusion or superdiffusion.

The results for the PDF also indicate that the superdiffusive motion we observed is not attributable to Lévy statistics. As plotted in Fig. 3, the data fall on a straight line when graphed with a logarithmic vertical axis and a horizontal axis representing squared displacement. This result shows that the PDF is Gaussian. Lévy statistics, where large displacements happen frequently and can be a possible cause of superdiffusion, can be excluded here because the PDF is not a power law as would be expected for Lévy statistics. One of the

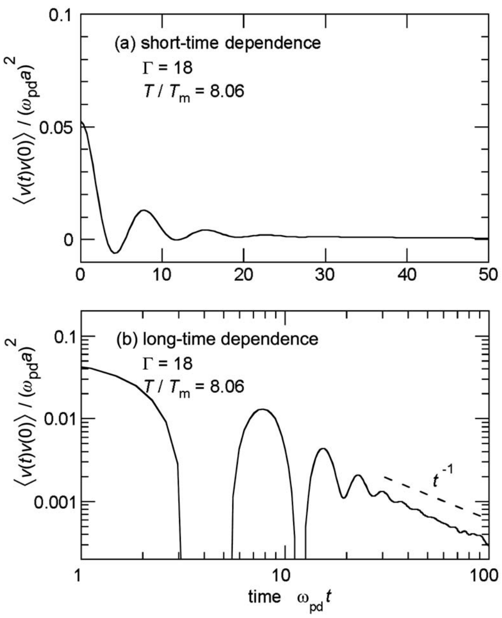

FIG. 4. Velocity autocorrelation function, VACF, shown with linear axes in (a) and log-log axes in (b). For the intermediate-temperature regime, the VACF decays as slowly as $1/t$, i.e., it has a long-time tail. This long-time tail indicates superdiffusion, and is considered to be a signature of mode coupling.

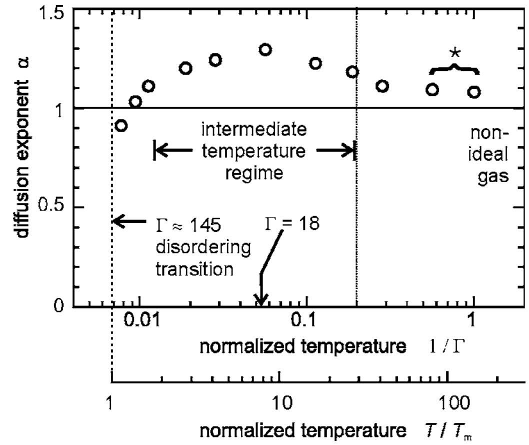

FIG. 5. Exponent α, computed from the MSD curve using Eq. (1). A value $\alpha > 1$ indicates superdiffusion, which occurs prominently in the intermediate-temperature regime. Data are also shown for colder and hotter regimes. Maximum superdiffusion occurs approximately at $\Gamma = 18$, where the viscosity happens to have a minimum [24,26]. The two data points indicated by the asterisk are less reliable than the others because the value of α is found by fitting a portion of the MSD curve which, for our simulation box size, is very limited. For low Γ, it is better to rely on the VACF.

experimental groups claiming to observe superdiffusion in a monolayer dusty plasma attributed their result to Lévy flights arising from a rotation of domains [17], which can occur under nonequilibrium conditions. This apparently did not occur in our equilibrium simulation.

Results for the VACF, Fig. 4, show a long-time tail in the VACF, indicating nondiffusive motion. The results are again for $\Gamma = 18$. We found that for large times, after the initial damped oscillations due to caged particle oscillating motion, the VACF decays as slowly as $1/t$. The long-time tail causes a divergence when attempting to calculate a diffusion coefficient using the Green-Kubo relation [28]. This divergence indicates superdiffusion.

B. Dependence on Γ

Varying the temperature, we found the dependence on Γ of the MSD results shown in Fig. 5. We always used the same time range, except for the two highest temperatures. The exponent α has its maximum value, indicating the most extreme superdiffusion, at $\Gamma \approx 18$. This result is significant because this happens at the same value of Γ where the viscosity was previously shown to have a minimum [24,26]. We performed our simulations for only one value of κ; in general, the value of Γ at the minimum viscosity depends slightly on κ [20].

Using the VACF, we found that at high temperatures the decay was much faster than $1/t$, indicating that either the motion is diffusive (or at least that any superdiffusion is not extreme). This diagnostic is especially useful at high temperatures because the portion of the MSD curve used for fitting the exponent α is limited for our simulation box size. Near the disordering transition the VACF is more difficult to interpret because it exhibits oscillations.

V. DISCUSSION

A $1/t$ long-time tail, as we have observed, for example, at $\Gamma = 18$, is a signature of mode-coupling in 2D equilibrium liquids. According to the mode-coupling theory, fluctuations decay into pairs of hydrodynamic modes [9]. The hydrodynamic modes affect the tail of the VACF. Our finding a lack of Lévy statistics indicates that the modes do not consist primarily of zero-frequency counter-rotating vortices.

Additionally, we report the result that the superdiffusion and long-time tails are most extreme for the condition where the viscosity has a minimum. For all liquids a coupling between diffusion and viscosity is expected, and for many liquids this is manifested by a Stokes-Einstein relation [23], although the Stokes-Einstein relation does not occur here because the motion is nondiffusive. Nevertheless, a relationship between random motion and viscosity is revealed here, by the coincidence of a minimum viscosity and maximum superdiffusion.

We thank Z. Donkó, V. Nosenko, and F. Skiff for helpful discussions. This work was supported by NASA and DOE.

[1] C. C. Grimes and G. Adams, Phys. Rev. Lett. **42**, 795 (1979).
[2] P. L. Gammel, D. J. Bishop, G. J. Dolan, J. R. Kwo, C. A. Murray, L. F. Schneemeyer, and J. V. Waszczak, Phys. Rev. Lett. **59**, 2592 (1987).
[3] A. A. Abrikosov, Sov. Phys. JETP **5**, 1174 (1957).
[4] C. A. Murray, W. O. Sprenger, and R. A. Wenk, Phys. Rev. B **42**, 688 (1990).
[5] T. B. Mitchell, J. J. Bollinger, X.-P. Huang, W. M. Itano, and D. H. E. Dubin, Phys. Plasmas **6**, 1751 (1999).
[6] S. Nunomura, D. Samsonov, S. Zhdanov, and G. Morfill, Phys. Rev. Lett. **96**, 015003 (2006).
[7] Y. Maruyama and J. Murakami, Phys. Rev. B **67**, 085406 (2003).
[8] R. Brown, Edinburgh New Philosophical Journal **5**, 358 (1828).
[9] M. H. Ernst, E. H. Hauge, and J. M. J. Van Leeuwen, Phys. Rev. Lett. **25**, 1254 (1970).
[10] J. R. Dorfman and E. G. D. Cohen, Phys. Rev. Lett. **25**, 1257 (1970).
[11] B. J. Alder and T. E. Wainwright, Phys. Rev. A **1**, 18 (1970).
[12] R. Zangi and S. A. Rice, Phys. Rev. Lett. **92**, 035502 (2004).
[13] D. N. Perera and P. Harrowell, Phys. Rev. Lett. **81**, 120 (1998).
[14] M. M. Hurley and P. Harrowell, Phys. Rev. E **52**, 1694 (1995).
[15] P. J. Camp, Phys. Rev. E **71**, 031507 (2005).
[16] W. T. Juan and Lin I, Phys. Rev. Lett. **80**, 3073 (1998).
[17] S. Ratynskaia, K. Rypdal, C. Knapek, S. Khrapak, A. V. Milovanov, A. Ivlev, J. J. Rasmussen, and G. E. Morfill, Phys. Rev. Lett. **96**, 105010 (2006).
[18] U. Konopka, G. E. Morfill, and L. Ratke, Phys. Rev. Lett. **84**, 891 (2000).
[19] H. Ohta and S. Hamaguchi, Phys. Plasmas **7**, 4506 (2000).
[20] K. Y. Sanbonmatsu and M. S. Murillo, Phys. Rev. Lett. **86**, 1215 (2001).
[21] G. J. Kalman, P. Hartmann, Z. Donkó, and M. Rosenberg, Phys. Rev. Lett. **92**, 065001 (2004).
[22] P. Hartmann, G. J. Kalman, Z. Donkó, and K. Kutasi, Phys. Rev. E **72**, 026409 (2005).
[23] B. Liu, J. Goree, and O. S. Vaulina, Phys. Rev. Lett. **96**, 015005 (2006).
[24] B. Liu and J. Goree, Phys. Rev. Lett. **94**, 185002 (2005).
[25] T. J. Feder, I. Brust-Mascher, J. P. Slattery, B. Baird, and W. W. Webb, Biophys. J. **70**, 2767 (1996).
[26] Z. Donkó, J. Goree, P. Hartmann, and K. Kutasi, Phys. Rev. Lett. **96**, 145003 (2006).
[27] B. J. West and W. Deering, Phys. Rep. **246**, 1 (1994).
[28] J.-P. Hansen and I. R. McDonald, *Theory of Simple Liquids*, 2nd ed. (Elsevier-Academic, San Diego, 1986).